INFLUENCE OF GAS SEALS ON ROTOR STABILITY OF A HIGH SPEED HYDROGEN RECYCLE COMPRESSOR

by

Kenneth E. Atkins

Senior Project Engineer

Engineering Dynamics, Incorporated

San Antonio, Texas

and

Robert X. Perez

Reliability Engineer

Champlin Refining Company

Corpus Christi, Texas

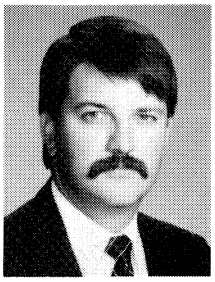

Kenneth E. Atkins is a Senior Project Engineer with Engineering Dynamics, Incorporated, and has experience in performing lateral and torsional critical speed analyses, rotor stability analyses and the evaluation of structural vibration problems using finite element methods. He has been actively involved in field troubleshooting of a wide variety of rotordynamics, structural and piping vibrations.

Mr. Atkins received a B.S. degree in Engineering Science from Trinity University in 1978. He is a member of ASME and a Registered Professional Engineer in the State of Texas.

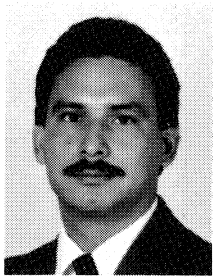

Robert X. Perez is a Reliability Engineer at the Champlin Refining Company, Corpus Christi Refinery. In addition to his reliability engineering duties, he serves as a Plant Specialist in the area of machinery monitoring. For the past six years, he has worked with the refinery's predictive maintenance group in solving plant machinery vibration problems. He has also worked to improve the refinery's machinery analysis and monitoring capabilities through the use of improved diagnostic equipment and techniques.

Mr. Perez is a Registered Professional Engineer in the State of Texas and a member of ASME and the Vibration Institute. He received his BSME degree from Texas A&M University and a MSME degree from the University of Texas.

ABSTRACT

A gas seal retrofit project for a 2800 hp, 10200 rpm, five-stage hydrogen recycle compressor is described. This barrel-type compressor operates with a 1205 psia suction pressure and 1490 psia discharge pressure. The unit is directly driven by a steam turbine through a continuously lubricated gear-type coupling. The gas seal retrofit project was initiated as a solution to a rotordynamic instability problem experienced on the compressor. The rotordynamic analysis showed that the rotor system stability would be improved with the gas seals. The other advantages of gas seals were considered as secondary to the stability improvements.

INTRODUCTION

The compressor was first commissioned in 1976 and operated with reasonable success for several years in the 7500-9500 rpm speed range. On several occasions during 1985 and 1986, high vibration levels were noticed in conjunction with short term operation above 10,000 rpm.

Without analyzing the vibration signals, the higher vibration levels at higher speeds were originally assumed to be unbalance related. However, an overspeed and coastdown test conducted in May, 1988 revealed a subsynchronous vibration component at speeds above 10,000 rpm, indicating an instability problem.

Higher unit charge rates in mid 1986 led to higher flow requirements for the recycle compressor. For this reason, continuous operation near 10,000 rpm was required and periodic excursions in the 10,500-11,000 rpm range were expected. On November 15, 1986, after the ambient temperature dropped below 50°F, shaft vibration levels of 2.0-3.0 mils were noticed on the local monitors. During the week of November 24, 1986, the compressor oil seals failed. The seals and the outboard bearing were replaced. Upon startup, high subsynchronous vibration levels were experienced. At this point, detailed field vibration measurements were made and a comprehensive rotordynamics analysis was initiated to characterize the problem and develop a solution.

FIELD VIBRATION MEASUREMENTS

Online Testing

A sketch of the steam turbine driven compressor train is shown in Figure 1. The compressor is equipped with radial proximity probes, two near each bearing mounted 45 degrees from vertical, 90 degrees apart. A set of baseline vibration spectra was obtained following the November, 1986 outage with the compressor operating at 8806 rpm (Figure 2). Significant subsynchronous vibration amplitudes occurred at approximately 4320 cpm (0.49 × running speed). On the compressor inboard end, the amplitude of the subsynchronous component exceeded that of the synchronous (unbalance related) vibration.

Because the compressor had recently been repaired, the possibility of a mechanical assembly problem resulting in a rub was considered. Typically, a mechanical rub produces nonsynchronous vibration components with a characteristic backward whirl orbit. The inboard proximity probe signals were band pass filtered

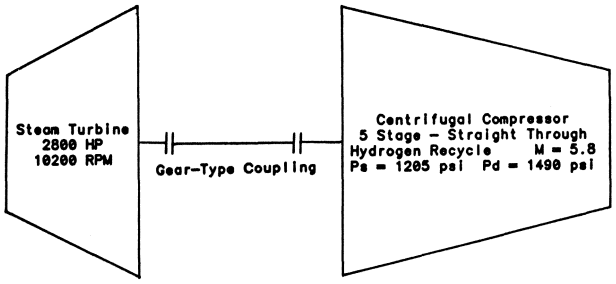

Figure l. System Schematic.

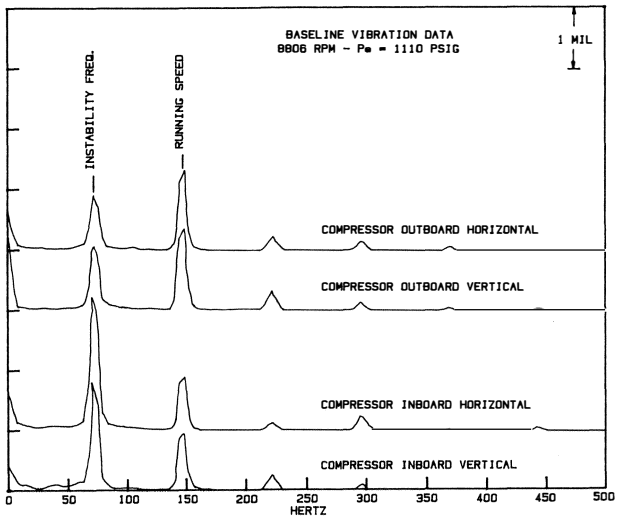

Figure 2. Baseline Vibration Data.

(10-100 Hz) and the subsynchronous orbit (Figure 3) showed that the whirl direction was forward, indicating that the problem was associated with a rotor-bearing system instability.

The unit speed was reduced to approximately 7000 rpm and vibration data were recorded as the unit speed was increased to 8800 rpm. A cascade plot of the compressor inboard proximity probe signals was generated during this speed run (Figure 4). This showed that the subsynchronous component became well defined near 8000 rpm and tracked running speed up to 8800

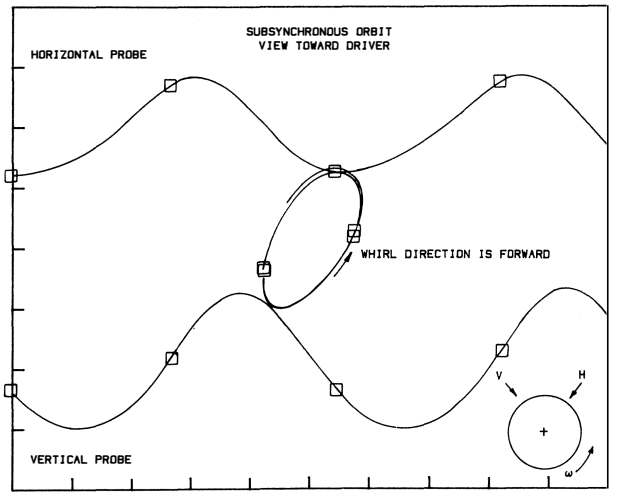

Figure 3. Subsynchronous Orbit Showing Forward Whirl.

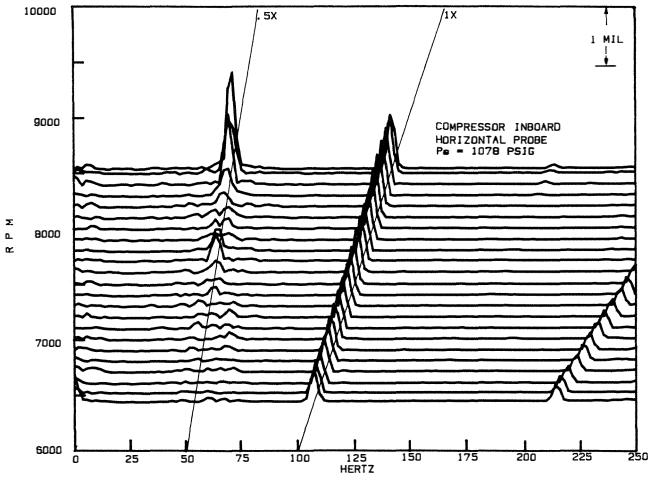

Figure 4. Cascade Plot at Suction Pressure = 1078 PSI.

rpm. The speed was limited to 8800 rpm because of the vibration levels.

Centrifugal compressors of this type are subjected to various destabilizing mechanisms including oil ring seals, interstage labyrinth seals, balance piston effects, and aerodynamic cross coupling at the compressor wheels. The aerodynamic cross coupling at the compressor wheels was thought to be minimal, since this was a low ratio machine compressing a light gas. Based on the authors' experience and discussions with the compressor manufacturer, the oil ring seals were thought to have the most significant effect on the system stability. This was further evaluated during the rotordynamics analysis.

Oil ring seals are generally designed to orbit with the shaft (float radially) so that the oil film forces developed between the shaft and the seal ring are negligible. However, if the seal rings lockup, then significant oil film forces, and, therefore, dynamic coefficients (similar to bearing coefficients), can be produced. Oil ring lockup has been discussed in the literature and considerable design effort is expended to prevent its occurrence. Allaire [1] and Kirk [2] describe this phenomenon and include calculation procedures and design considerations to predict and prevent seal ring lockup.

In general, if the seal rings are locked, the rotor is supported both by the bearings and by the seals. That is, the seals will have a set of dynamic stiffness and damping coefficients as do the bearings. Typically, the direct stiffness and damping terms at the seals are much lower than the bearing direct stiffness and damping terms. Allaire and Kocur [1] observed that oil seal cross coupled coefficients can be significant since tilting pad bearings typically have low cross coupled coefficients. Calculations of the seal ring coefficients show that the cross coupled terms are usually higher as the seal eccentricity ratio is increased. The minimum cross coupling occurs at zero eccentricity (centered seals). For this reason, the "soft start" described by Kirk [2] was executed in the field as an attempt to provide a short term solution while the stability analysis was performed to design a long term fix.

The "soft start" involved reducing the compressor speed to approximately 7000 rpm and reducing the suction pressure to the minimum possible value of 914 psig. As the speed increased, the instability frequency component did not limit the compressor speed due to vibration until about 9900 rpm, as shown in Figure 5. The speed run was then repeated with the suction pressure set at approximately 1200 psig. The compressor speed could be increased to 9600 rpm without the subsynchronous component exceeding the 1 × vibration or causing a vibration alarm (Figure

6). At this suction pressure, the speed was limited to 9600 rpm because of the steam turbine horsepower. The soft start tests verified that the oil ring seals were a significant influence on rotor stability.

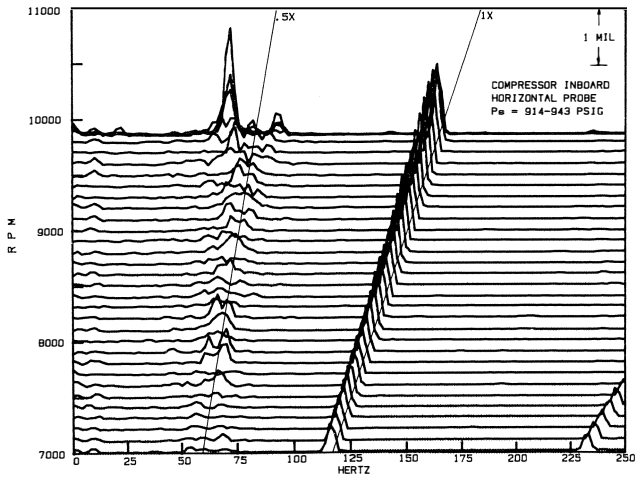

Figure 5. Cascade Plot at Reduced Suction Pressure.

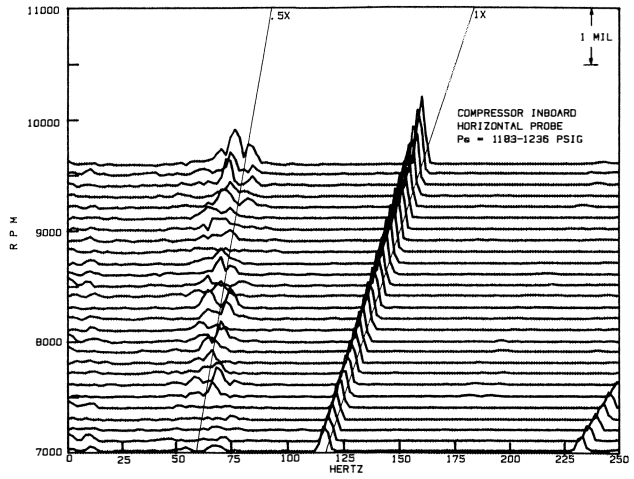

Figure 6. Cascade Plot at High Suction Pressure.

As the machine operated, the vibration levels continued to fluctuate due to the instability component. The vibration levels were controlled by limiting the compressor speed until a design change could be implemented during the scheduled turnaround in May 1987.

Impact Tests of Spare Rotor

Detailed dimensioned drawings of the rotor were not available for the rotordynamics model; therefore, dimensions were taken from the spare rotor in storage at a local maintenance shop. Additionally, the spare rotor was weighed and impact tested in the free-free condition for the purpose of verifying the computer model.

Test points were chosen at 15 points along the length of the shaft for acquiring impact mode shape data. The rotor was suspended vertically by a nylon sling to approximate the free-free condition and impacted at the selected test points using an instrumented hammer. Transfer function spectra were obtained from the impact and reference accelerometer signals and stored for each location. From this data, natural frequencies and mode shapes could be determined. The overall transfer function spectrum showing the natural frequencies for the rotor is shown in Figure 7. This is an envelope of the 15 spectra obtained from the impact test. The mode shape data is presented in the next section in comparison with the calculated results.

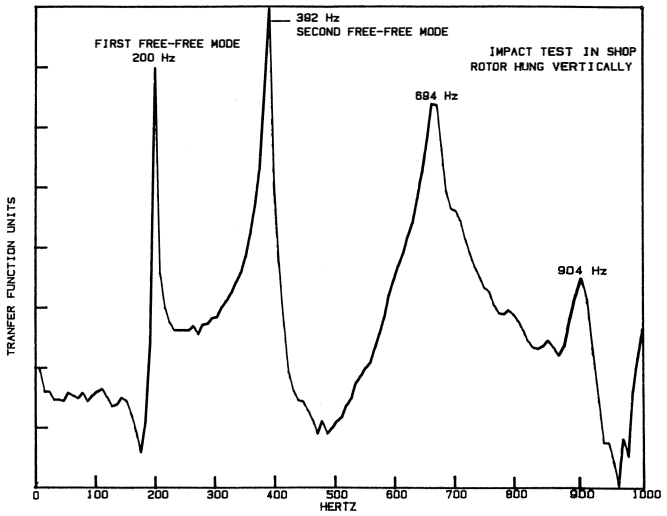

Figure 7. Impact Test Response Spectrum.

ROTORDYNAMICS ANALYSIS

Undamped Critical Speed Calculations

The first step in the rotordynamic analysis was to develop the undamped critical speed map (Figure 8) for comparison to the impact tests. At relatively low values of support stiffness ($< 10^4$ lb/in) mode numbers, 3 and 4 represent the first two free-free modes of the rotor. These can be compared to the first two measured natural frequencies. The calculated third mode (Figure 9) for a low support stiffness value (1000 lb/in) was 11730 cpm, which corresponds to the measured first free-free mode at 12000 cpm (Figure 10). The calculated frequency is within 2.3 percent of the measured frequency.

The model was further verified by comparing the calculated fourth mode at low stiffness to the measured second free-free mode. These results are presented in Figures 11 and 12. Again, the mode shapes agreed closely and the calculated frequency

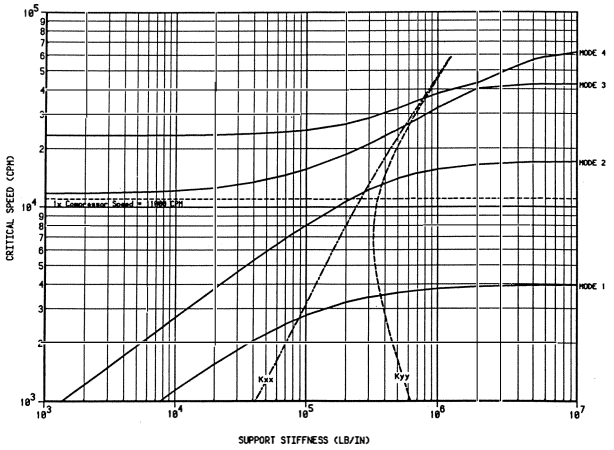

Figure 8. Undamped Critical Speed Map.

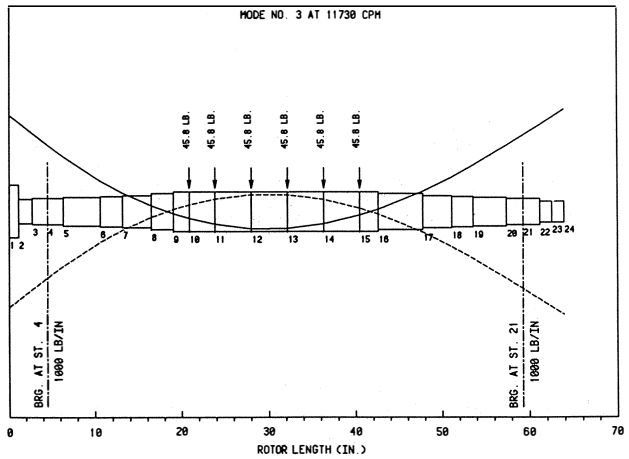

Figure 9. Calculated First Free-Free Mode.

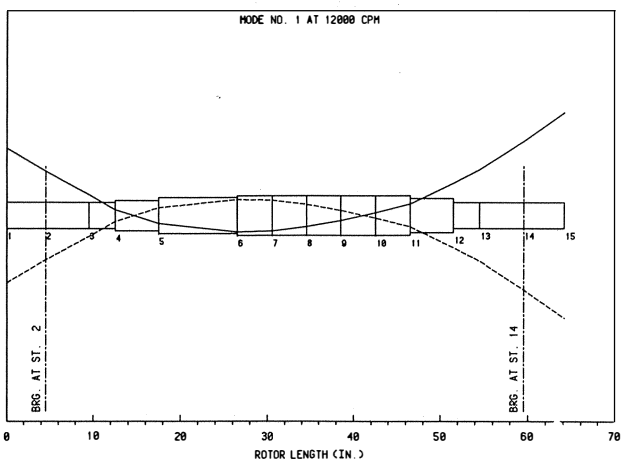

Figure 10. Measured First Free-Free Mode.

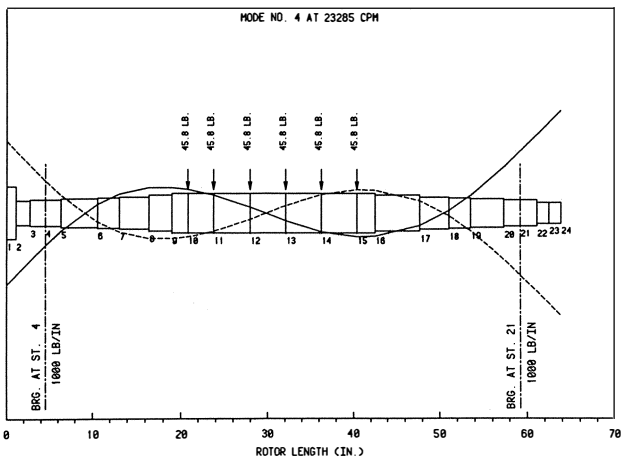

Figure 11. Calculated Second Free-Free Mode.

(23285 cpm) was within one percent of the measured value (23520 cpm).

Based on these comparisons, the rotor model was felt to be adequate for the purposes of the rotordynamics analysis. The next step was to compute the dynamic fluid film coefficients for the tilt pad bearings, oil ring seals, and labyrinth seals.

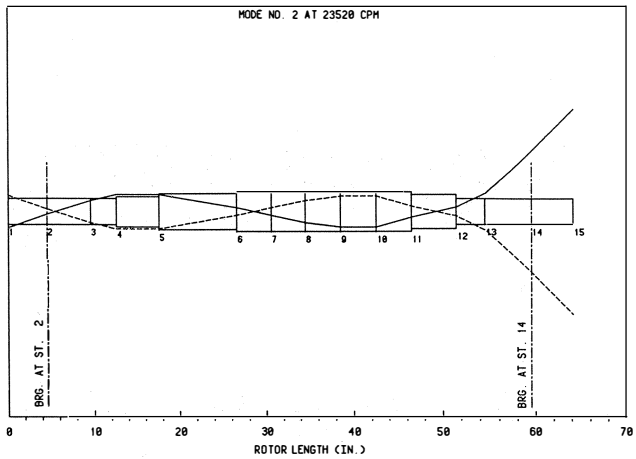

Figure 12. Measured Second Free-Free Mode.

Bearing and Seal Coefficients

The original compressor design included the use of five shoe, load-on-pad (5SLOP) tilt pad bearings. The bearing coefficients were calculated for nominal clearance and preload based on the manufacturer's specified tolerances (Table 1).

Table 1. Original Bearings for Hydrogen Recycle Compressor Assembled Diametrical Clearance = 5 mils Preload = 0.412 Mu = 2.0 × 10^{-6} reyns

Speed (rpm)	Kxx (lb/in)	Kyy (lb/in)	Cxx (lb-s/in)	Cyy (lb-s/in)
6000	1.608×10^5	3.288×10^5	3.508×10^2	5.225×10^2
7000	1.809×10^5	3.264×10^5	3.436×10^2	4.739×10^2
8000	2.009×10^5	3.283×10^5	3.382×10^2	4.395×10^2
9000	2.207×10^5	3.349×10^5	3.342×10^2	4.169×10^2
10000	2.404×10^5	3.428×10^5	3.306×10^2	3.977×10^2
11000	2.603×10^5	3.532×10^5	3.280×10^2	3.837×10^2
12000	2.803×10^5	3.659×10^5	3.261×10^2	3.740×10^2

The floating oil ring seal design is shown in Figure 13. The pressure breakdown from approximately suction pressure to atmospheric pressure occurs across the three rings shown. The first ring is a plain bushing secured by an axial pin. The second and third rings are circumferentially grooved and have radial anti-rotation pins. Pertinent seal dimensions and fluid properties are given on the figure.

The analysis considered two cases initially. First, the seal rings were assumed to float freely, in which case the dynamic coefficients would be negligible. This "floating ring" assumption is, therefore, the same as analyzing the rotor without seal effects. When this assumption is made, the rotor response and stability are independent of the seal design parameters (length, diameter, clearance, pressure drop, etc.).

If the seal rings do not float freely, then the second situation arises in which fluid film coefficients (similar to bearing coefficients) must be computed for the seals. This is also referred to as the "locked seal" assumption. For this "locked seal" case, the stiffness and damping coefficients are further dependent on assumptions for lockup position (eccentricity and attitude angle) and speed. Generally speaking, the destabilizing cross coupled stiffness terms (Kxy and Kyx) increase for higher values of eccentricity.

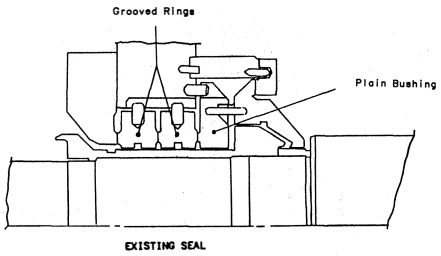

Seal Dimensions

Component	Diameter (in)	Length (in)	Diametrical Clearance (in)
Stationary Bushing	4.0	0.703	0.0075
Floating Rings	4.0	0.400 (Per Land)	0.0075

Fluid Properties at 140°F

Density = 3.10×10^{-2} lb/in^3 Absolute Viscosity = 1.71 μ reyns

Pressure Drop = 1078 psi (Total Across Seal)

Figure 13. Original Oil Ring Seal Design.

The labyrinth seals at the impellers and balance piston can influence the rotor stability as well as the oil ring seals [3-7]. These effects are considered in the analysis by calculating the labyrinth stiffness and damping terms for application to the rotor model just as the bearing and oil ring seal coefficients are treated. The destabilizing cross coupled stiffness terms and the stabilizing direct damping are again the primary factors.

The balance piston was thought to be the most significant of the labyrinth seals, since it is the longest seal with the highest Δp (Figure 14). A comparison of the calculated balance piston coefficients [3] at 10,000 rpm with those for the bearings and oil ring seals is given in Table 2. The cross coupled stiffness and direct damping values calculated for the centered (zero eccentricity) oil ring seals were significantly higher than those for the balance piston. This will be discussed further in the following section on rotor stability. The primary direct stiffness (Kxx and Kyy) occurs at the bearings, with negligible direct stiffness at the oil ring seals and negative values at the balance piston.

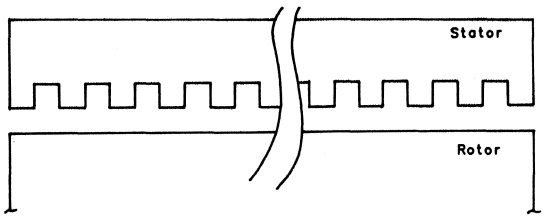

Balance Piston Labyrinth Seal

Teeth on Stator — 24 Teeth — 0.023″ each

Tooth Pitch = 0.144″ **Tooth Depth = 0.125″**

Radial Clearance = 10–12 mils **Length = 3.335″**

Bore = 8.21″ $\nu = 7.073 \times 10^{-4}$ in^2/sec **M = 5.8**

$Z_s = 1.024$ $P_s = 1205$ psia $T_s = 102$°F

$Z_D = 1.033$ $P_D = 1490$ psia $T_D = 134$°F

$C_p/C_v = 1.38$ R = 266.4 ft-lb/lb-mole-°R

Figure 14. Balance Piston Labyrinth Seal.

Table 2. Comparison of Fluid-Film Stiffness and Damping Coefficients for Bearings, Oil Seals, and Balance Piston Labyrinths

	Coefficients Calculated at 10,000 rpm							
	Stiffness Values — lb/in				Damping Values — lb-sec/in			
Location	Kxx	Kxy	Kyx	Kyy	Cxx	Cxy	Cyx	Cyy
Nominal 5SLOP Bearings	2.40 $\times 10^5$	0	0	3.43 $\times 10^5$	331	0	0	398
Nominal Oil Ring Seals (Centered)	5	5.54 $\times 10^6$	−5.54 $\times 10^6$	5	10589	2.9	−2.9	10589
Balance Piston Labys (0.8 Preswirl)	−14800	8260	−8260	−14800	12.4	11.5	−11.5	12.4

Stability Analysis

The rotor stability was calculated using the bearing and seal coefficients in conjunction with the rotor model. The stability analysis calculates the system damped natural frequencies as opposed to the undamped natural frequencies computed for the critical speed map. The solution to the equations of motion for damped free vibration yields a set of complex frequencies or damped eigenvalues of the form:

$$s = \lambda + i\omega$$

where

s = complex frequency
λ = damping exponent
ω = damped natural frequency
i = $\sqrt{-1}$

The stability of rotor systems is generally expressed in terms of the logarithmic decrement or "log dec." The log dec is essentially a measure of system damping. In mathematical terms, the log dec is defined as:

$$\delta = \frac{-2\pi\lambda}{\omega}$$

Theoretically, a positive log dec indicates a stable system and a negative log dec indicates an unstable system. Because of uncertainties involved with rotor stability calculations, the authors have found that calculated log dec values of 0.1 or greater (with all destabilizing mechanisms considered) are desired to ensure a stable system. Rotors with calculated log dec values less than 0.1 are considered marginally stable and can be sensitive to small changes in system parameters such as bearing clearance and preload, seal clearance and eccentricity, labyrinth seal clearances, etc.

In addition to the oil seal and balance piston labyrinth effects discussed in the previous section, the rotor system is also subject to destabilizing forces at the impellers, which is usually referred to as "aerodynamic loading." Various methods of calculating this effect have been discussed in the literature [8-10]. The approach for this analysis was to consider these effects in the context of the measured rotor behavior.

The actual value of aerodynamic loading was predicted according to the equation proposed by Wachel [8].

$$Kyx = \frac{-6300\ HP}{NDh}\left(\frac{\rho_d}{\rho_s}\right)$$

where

Kyx = Aerodynamic Cross Coupling (lb/in)
M = Molecular weight of gas (dimensionless)
HP = Compressor Horsepower (hp)
N = Compressor Speed (rpm)

D = Impeller Diameter (in)
h = Minimum Flow Restriction (in)
ρ_d = Discharge Density (lb/in^3)
ρ_s = Suction Density (lb/in^3)

The predicted aerodynamic loading for this machine was −740 lb/in. This is a relatively low value of aerodynamic loading, which is to be expected, since this is a low pressure ratio machine compressing a light gas. The system log dec was mapped *vs* aerodynamic loading at constant speed (10,000 rpm) to determine the sensitivity to this parameter. The results for the following three cases were plotted (Figure 15):

- Rotor 5SLOP tilt pad bearings only
- Rotor with 5SLOP bearings and zero eccentricity (centered) oil ring seals
- Rotor with 5SLOP bearings, oil seals, and balance piston labyrinths.

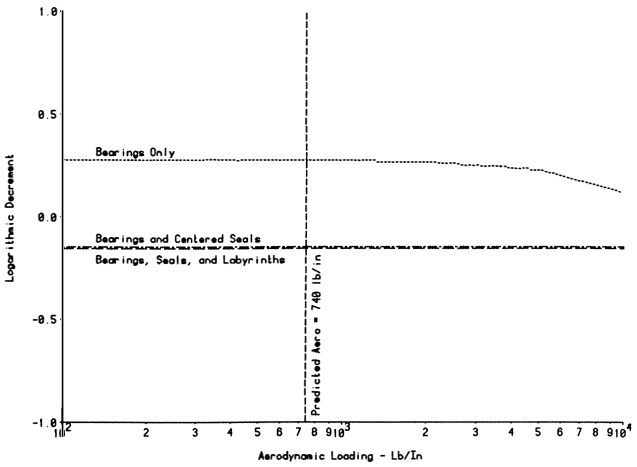

Figure 15. Logarithmic Decrement vs *Aerodynamic Loading.*

This plot showed that the system log dec was not sensitive to aerodynamic loading in the range of the predicted value for any of the three cases considered.

Another significant conclusion drawn from this plot was that the balance piston labyrinths had little effect on the rotor stability. The dominant influence which caused the log dec to change from positive (stable) to negative (unstable) was the oil ring seals. This was true for zero eccentricity (centered) seals and would be even more dominant with increased seal eccentricity.

In order to compare the calculated and measured vibration data, the system log dec was calculated as a function of speed with locked (centered) oil ring seals and the predicted aerodynamic loading load applied at the impellers. The calculated instability frequency and log dec *vs* speed were superimposed on the measured data (Figure 16). This showed good correlation between the calculated and measured results.

It was evident that the primary destabilizing effect was the cross coupling generated by the oil seals under locked conditions. The compressor manufacturer proposed a seal modification to decrease the unbalanced axial forces on the seal faces and, thereby, reduce the tendency for the seals to lock up. It also incorporated a double groove design to reduce the cross coupled stiffness (Figure 17). Due to the critical nature of this machine, seal and bearing modifications were further investigated with the intent of designing a system that would remain stable even under locked conditions. A summary of the modifications analyzed is given in Table 3.

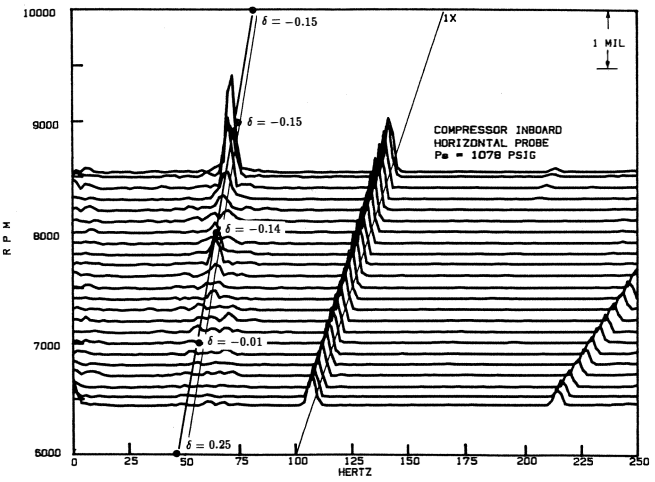

Figure 16. Comparison of Calculated and Measured Instability Frequency.

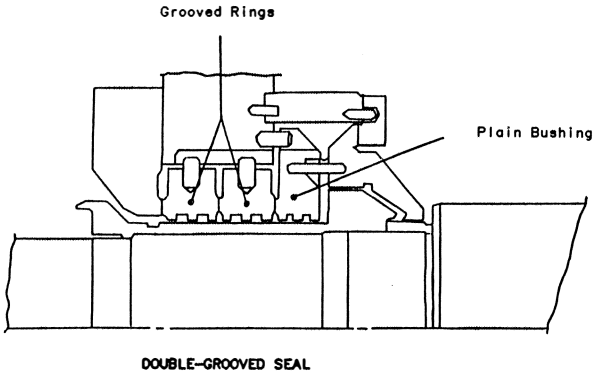

Figure 17. Double Grooved Oil Ring Seal.

Table 3. Summary of Designs Analyzed for Stability

Case	Description
1	Nominal Bearings, Floating Seals
2	Nominal Bearings, Nominal Seals
3	Nominal Bearings, Doubled Seal Clearance
4	Increased Bearing Clearance, Reduced Preload, Nominal Seals
5	Nominal Bearings, Removed Circumferential Grooves in Seal Rings
6	Modified Bearing as in Case 4, Doubled Seal Clearance
7	Nominal Bearings, Double Grooved Seal
8	Nominal Bearings, Double Grooved Seal with Doubled Clearances

For each of the designs described in Table 3, the damped natural frequencies and log dec were calculated *vs* speed with the aerodynamic loading held constant at the predicted value of 740 lb/in. The only cases for which the log dec remained positive throughout the 6000-12000 rpm range were cases 1 and 8 (Figure 18). Case 1 was the "floating ring" or no seal effect assumption and case 8 was the double grooved seal with doubled clearances. Based on this analysis, the options were:

- Rely on the proposed oil seal modifications to prevent oil seal lockup,
- Double the clearance of the modified seal to improve stability if lockup occurred, or
- Consider the use of gas seals, which achieve the same effect as the "floating ring" assumption.

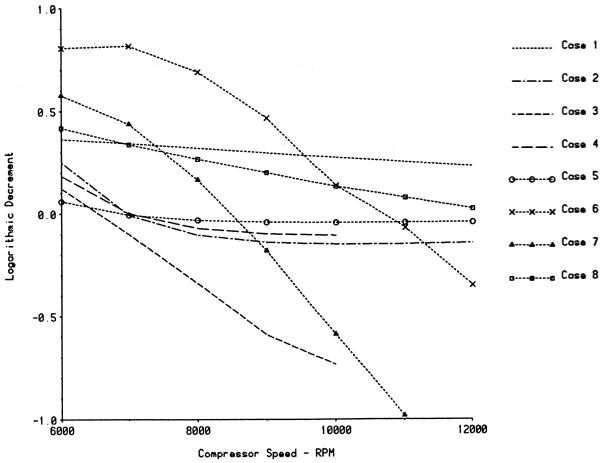

Figure 18. Logarithmic Decrement vs *Speed for Various Design Modifications.*

CONSIDERATION OF GAS SEALS FOR POSSIBLE RETROFIT

Discussion of this application with gas seal vendors indicated that they had no experience with gas seals in hydrogen service at these pressures and speeds. The authors were unable to identify an existing installation of gas seals in similar service. However, users were found with gas seals in hydrogen service. The maximum pressure hydrogen installation reviewed was 250 psi at 7500 rpm *vs* 1205 psi at 10,200 rpm in this application. Nonetheless, it was decided to pursue the gas seal design to examine the potential benefit.

Principles of Operation

The gas seal design considered consists of primary and secondary sealing stages (Figure 19) which are identical in design, and are capable of operating to differential pressures of 1200 psi and above. In normal operating conditions, all of the pressure breakdown takes place across the primary seal. If the primary seal fails, the full pressure breakdown will take place across the secondary seal. Either seal will operate alone as a backup to the other.

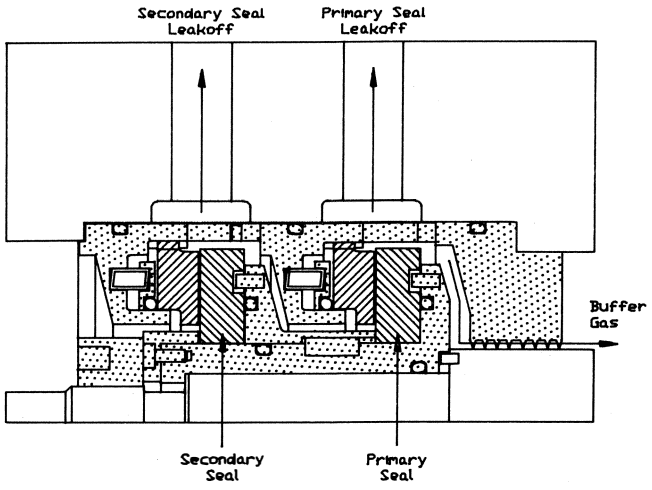

Figure 19. Gas Lubricated Face Seal Showing Buffer Gas and Seal Leakoff.

The seal is a noncontact end face seal that operates under balanced hydrostatic and hydrodynamic forces for sealing. At seal cavity pressures above 100 psi and 0 rpm, the seal faces will move apart 0.0001 in to 0.0002 in and reach hydrostatic equilibrium. Hydrodynamic force is generated mechanically by the rotation of the sealing ring. Spiral grooves are etched in the ring face (Figure 20), which acts as a small centrifugal pump designed with a high head, low flow characteristic. This pumping action creates a highly compressed film of gas which separates and cools the faces of the seal. The size of the gap between the faces is stabilized when the hydrostatic and hydrodynamic forces are equal. The portion of the sealing ring below the spiral grooves is the seal dam. The rotational speed at which the sealing rings separate and the size of the film/gap between the seal faces are determined by the face geometry. The face geometry design is based on the gas molecular weight, gas viscosity, rpm, and the forces generated by product pressure. The proposed gas seal was designed to lift off at approximately 150 rpm. The noncontact mode of operation results in lower power consumption (approximately 1.0 hp) which contributes to the longevity of the seal.

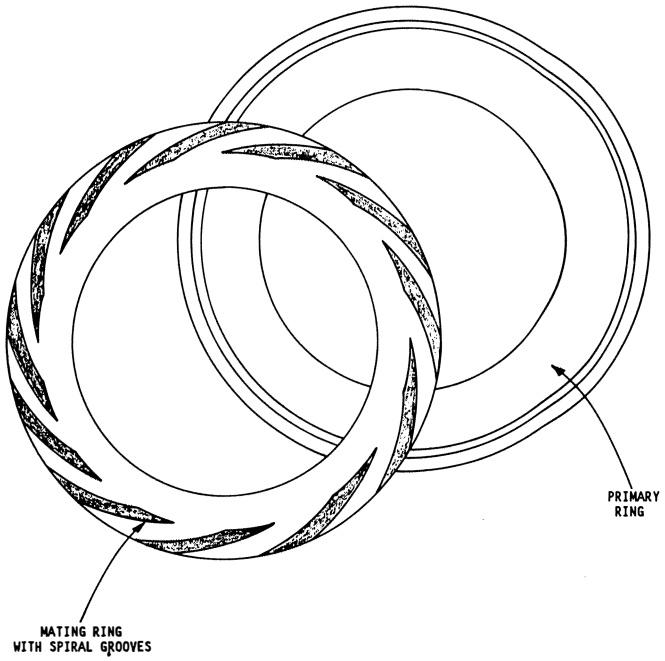

Figure 20. Surface Treatment of Primary and Mating Seal Rings.

Economics

Because the gas seal solution was the most costly of the alternatives, other economic advantages were considered. The economic evaluation conducted was based on the comparison of maintenance and operating cost for oil seals and gas seals. Some of the costs considered were:

- Maintenance costs/year
- Oil usage
- Parasitic horsepower
- Parasitic load of seal oil pumps
- Process gas leakage rate.

A detailed study of these costs revealed that significant savings were possible with gas seals. Because these savings represented a project payback of one to two years, it was agreed that the project could be justified on these economics alone. How-

ever, because the primary purpose in using gas seals was to eliminate cross coupling effects and gain rotor stability, the favorable economics of gas seals was simply an added benefit of the retrofit. Based on the numerous advantages of the gas seals over the oil seals and the favorable user experience of gas seals in hydrogen service, approval was given for installing the gas seals.

Design of Gas Seal System

The main concern during the initial design phase of the gas seals was obtaining accurate stuffing box dimensional data. Since the gas seal was being purchased from a third party, the compressor manufacturer had to provide the needed dimensional data. Since neither dimensional drawings nor a spare compressor were available for measurements, the original equipment manufacturer (OEM) was the only available source for this information. This information was critical because if the gas seal cartridge did not fit properly, the planned unit outage could be extended.

The compressor manufacturer worked with the user and the gas seal manufacturer to provide all the necessary gas seal envelope dimensions. Seal cavity and shaft dimensional information was reviewed by the gas seal manufacturer and compared with the proposed gas seal design to ensure the dimensional integrity of the overall retrofit design. Cooperation and communication between the OEM, gas seal manufacturer and end user is essential in ensuring the successful retrofit of a third party gas seal.

Auxiliary Seal Piping

Once the seal cavity dimensional information was obtained and the seal design, the auxiliary seal piping design began. The auxiliary seal piping consists of (Figure 21):

- Filtered buffer gas piping (A)
- Primary seal leakoff piping and (B)
- Secondary seal leakoff piping (C).

Filtered buffer gas is taken off the compressor discharge line and is injected upstream of the primary seal in order to provide a clean seal medium for the primary seal. The leakage across the primary seal is piped from the interstage seal cavity to the flare

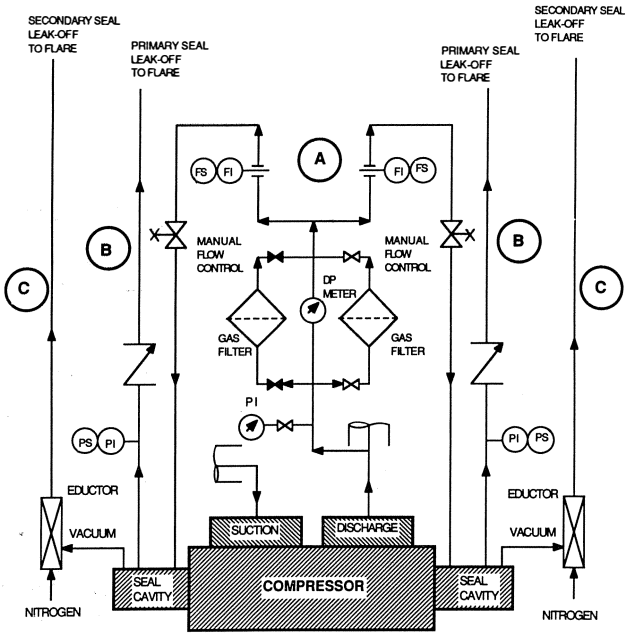

Figure 21. Gas Seal System Auxiliary Piping.

in order to maintain a low (0-2 psig) pressure between the primary and secondary seals. This means that the primary seal has a 1200 psi differential and 1.0 to 2.0 scfm leakage rate under normal conditions, while the secondary seal will have a pressure drop of only a few psi.

A critical aspect of the auxiliary seal piping is the associated instrumentation. Operations personnel must rely on this instrumentation to determine the condition of the gas seal faces. A listing of all the seal gas alarms is included in Table 4. The two most important alarms are (1) buffer gas flow and (2) primary seal leakoff gas flow. If buffer gas flow is lost, the possibility of reverse flow exists. In this case, unfiltered process gas will flow across the seal faces, possibly causing damage. For this reason, an alarm was set up to alert operations personnel of buffer gas flow below 4.0 scfm.

Table 4. Seal Gas Alarms

Buffer gas flow	2	These alarms signal the condition of low gas flow to the primary seals. A flow of less than 4 scfm triggers these alarms
Primary seal leakoff flow	2	These alarms signal the condition of high primary leakoff flows. A flow of greater than 8 scfm triggers these alarms
Intermediate seal	2	If excessive primary seal leakage occurs, the intermediate cavity will pressure up. These alarms are set at 50 psi. These cavities normally run at 0-2 psig.
Secondary seal cavity pressure	2	If both primary and secondary seals leak excessively, this cavity will pressure up. These alarms are set at 25 psig. These cavities normally run at 0 psig.
Buffer gas filter Δp	1	If the buffer gas filter plugs, this alarm will go off. This alarm is set at 10 psig.

Probably the most important measured seal gas parameter is that of primary seal leakoff flow. Under normal conditions, about 1.0 scfm is expected. If seal face damage is experienced, this flow will increase. A primary seal leakoff flow greater than 8.0 scfm will signal a seal problem. The primary seal leakoff rate is constantly monitored in order to spot any upward trends. Even though the secondary seal will allow continued operation in the event of a primary seal failure, extended operation in this manner is not recommended. Spotting an upward trend in primary seal leakoff flow before levels are excessive is vital to ensure a safe outage and a timely repair.

Under normal conditions, the secondary seal sees a 0-2.0 psi differential pressure. With this type of Δp, about 0.05 scfm continuous leakage is expected across the secondary seal. Because of the possibility that this continuous leakage might develop into an emission problem, it was decided to incorporate an eductor system downstream of the secondary seal. This system includes nitrogen powered venturis, which maintain a slight vacuum downstream of the secondary seals and preclude atmospheric leakage.

Installation

The gas seal cartridges were installed during a planned unit outage in May 1987. The installation took approximately three days with some delays due to minor dimensional differences between the seal cavity and the seal cartridges.

After installation, the seals were tested by pressurizing the compressor to about 400 psi using nitrogen. Once this pressure was obtained, the compressor shaft was rotated by hand. The pressure was held for over an hour and then released. During

this time, no pressure was lost. This proved that all the O-rings were sealing and that the seal faces were properly aligned.

OPERATION OF COMPRESSOR WITH GAS SEALS

The compressor was first started with the gas seals on May 21, 1987. The unbalance response peak (first critical speed) was measured as 3750 cpm (Figure 22), which was in reasonable agreement with the predicted value of 3600 cpm (Figure 23). A cascade plot of the speed run from approximately 6400-9200 rpm (Figure 24) showed that the stability threshold had increased as predicted, since no significant subsynchronous vibration levels occurred. The calculated damped natural frequency and corresponding log dec *vs* speed are superimposed on the cascade plot, which does show some small vibration amplitudes in the predicted frequency range.

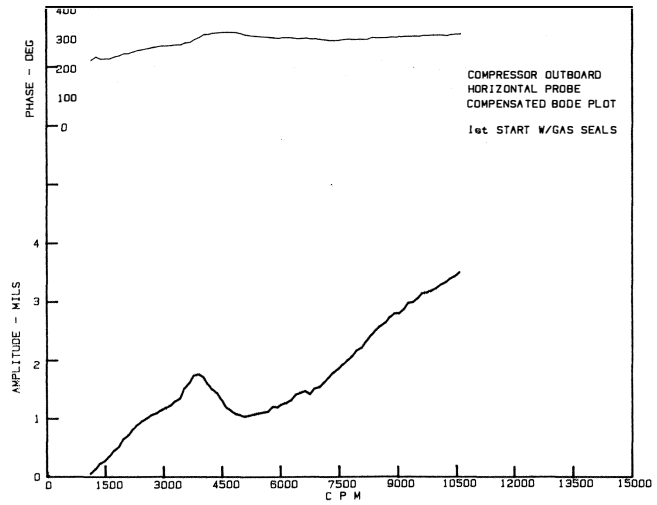

Figure 22. Measured Unbalance Response with Gas Seals Installed.

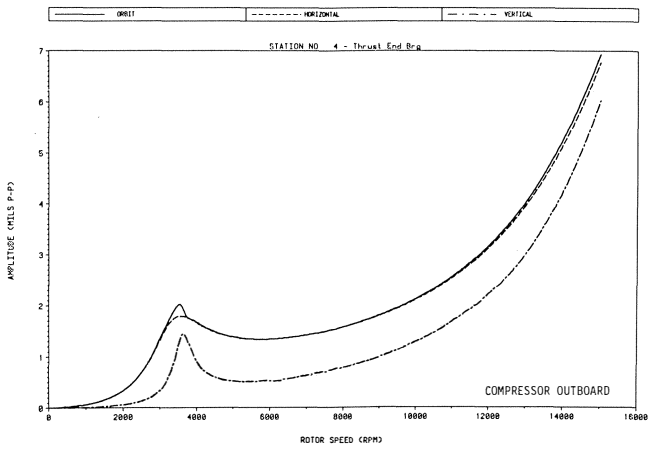

Figure 23. Predicted Unbalance Response with Gas Seals Installed.

A final speed test was conducted with the maximum available suction pressure (1240 psi) to confirm that the rotor remained stable with the unit at full operating conditions (Figure 25). The stability threshold remained above the maximum obtainable speed, which was 9500 rpm at this suction pressure. The subsynchronous vibration levels were again low, with some broad band response near the calculated first forward whirl frequency.

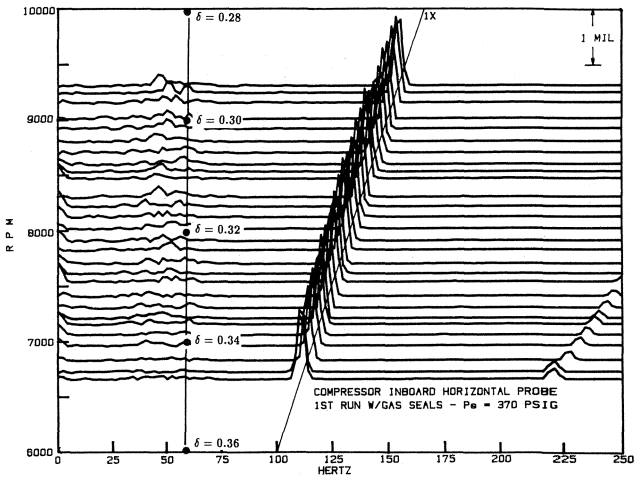

Figure 24. Comparison of Calculated and Measured Instability Frequency with Gas Seals.

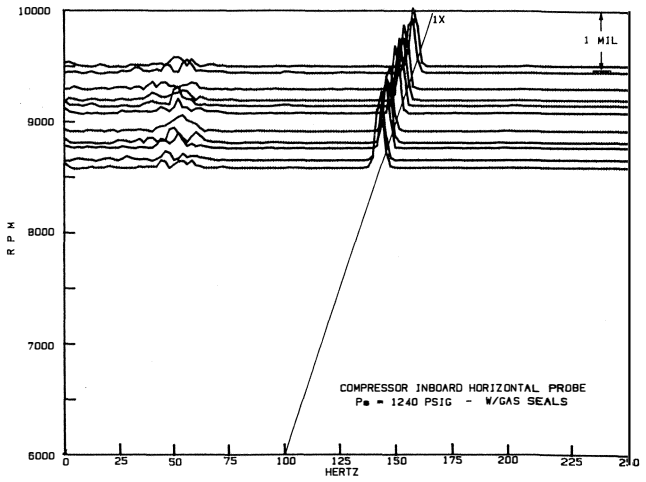

Figure 25. Cascade Plot at High Suction Pressure with Gas Seals.

CONCLUSIONS

The data presented here have demonstrated the significance of oil ring seals on rotor stability. For compressors of this type, with light gas service and low head rise, the oil ring seals can dominate the destabilizing forces in relation to the aerodynamic loading and labyrinth seal effects. This was shown to be true even for low eccentricity ratios (centered seals).

The advent of gas lubricated face seals capable of performing in this service provides the designer with another option for minimizing the destabilizing mechanisms and, therefore, improving machinery reliability. Care must be taken in the application of gas seals, as others have concluded in other applications that damping from the oil seals can improve rotor stability. A careful rotordynamics evaluation is necessary whenever gas seals are to be utilized.

REFERENCES

1. Allaire, P. E. and Kocur, J. A., "Oil Seal Effects and Subsynchronous Vibrations in High-Speed Compressors," Instability in Rotating Machinery NASA Conference Publication 2409, Carson City, Nevada (June 1985).
2. Kirk, R. G., "Oil Seal Dynamics: Considerations for Analysis of Centrifugal Compressors," Proceedings of the 15th Turbomachinery Symposium, Turbomachinery Laboratory, Department of Mechanical Engineering, Texas A&M University, College Station, Texas, pp. 25–34 (1986).
3. Scharrer, J. K., "A Comparison of Experimental and Theoretical Results for Labyrinth Gas Seals," Ph.D. Dissertation, Texas A&M University, College Station, Texas (1987).
4. Childs, D. W., and Scharrer, J. K., "Experimental Rotordynamic Coefficient Results for Teeth-on-Rotor and Teeth-on-Stator Labyrinth Gas Seals," ASME International Gas Turbine Conference, Dusseldorf, West Germany, paper no. 86-CT-12 (1986).
5. Iwatsubo, T., Motooka, N., and Kawal, R., "Flow Induced Force of Labyrinth Seal," Proceedings of Rotordynamic Instability Problems in High Performance Turbomachinery, Texas A&M University, pp. 205-222 (1982).
6. Wright, D. V., "Labyrinth Seal Forces on a Whirling Rotor," Rotor Dynamical Instability, AMD Volume 55, Presented at the Applied Mechanics Engineering Conference, ASME, Houston, Texas (1983).
7. Wyssman, H. R., "Flow in Labyrinth Seals and Its Influence on Rotor Stability or Turbocompressors," Von Karman Institute for Fluid Dynamics, Lecture Series 1987-01 Flow in Centrifugal Compressors, Brussels, Belgium (1987).
8. Wachel, J. C., "Case Histories of Rotor Dynamic Instabilities in the Field," Short Course in Rotordynamics of Turbomachinery, Texas A&M University, (1981).
9. Kirk, R. G., and Donald, G. H., "Design Criteria for Improved Stability of Centrifugal Compressors," Rotor Dynamical Instability, AMD Volume 55, Presented at the Applied Mechanics Engineering Conference, ASME, Houston, Texas (1983).
10. Alford, J. J., "ProtectingTurbomachinery from Self-Excited Rotor Whirl," ASME Journal of Engineering for Power, *87*, (October 1965).
11. Kocur, J. A., Platt, J. P, and Shabi, L. G., "Retrofit of Gas Lubricated Face Seals in a Centrifugal Compressor," Proceedings of the Sixteenth Turbomachinery Symposium, Turbomachinery Laboratory, Department of Mechanical Engineering, Texas A&M University, College Station, Texas, pp. 77-83 (1987).
12. Allaire, P. E., Lee, C., and Furris, R., "Turbulent Flow in Seals: Load Capacity and Dynamic Coefficients," University of Virginia, Report No. UVA/464761/ME76/139 (1986).
13. Lund, J. W., "Stability and Damped Critical Speeds of a Flexible Rotor in Fluid Film Bearings," ASME Paper No. 73-DET-103, Design Engineering Technical Conference, Cincinnati, Ohio (1973).